

## Structures and Phase Transitions in $\text{Rb}_2\text{MoO}_4$ and $\text{Rb}_2\text{WO}_4$

Hirotake Shigematsu,<sup>1\*</sup> Keisuke Nomura,<sup>2</sup> Katsura Nishiyama,<sup>2</sup> Takeo Tojo,<sup>3</sup> Hitoshi Kawaji,<sup>3</sup> Tooru Atake,<sup>4</sup> Yukihiko Kawamura,<sup>5</sup> Tatsuki Miyoshi,<sup>6</sup> Yoshitaka Matsushita,<sup>7</sup> Masahiko Tanaka<sup>7</sup> and Hiroyuki Mashiyama<sup>6</sup>

<sup>1</sup>Faculty of Education, Yamaguchi University, 1677-1 Yoshida, Yamaguchi 753-8513, Japan

<sup>2</sup>Faculty of Education, Shimane University, 1060 Nishikawatsu-cho, Matsue 690-8504, Japan

<sup>3</sup>Materials and Structures Laboratory, Tokyo Institute of Technology, 4259 Nagatsuta-cho, Midori-ku, Yokohama 226-8503, Japan

<sup>4</sup>General Safety Management Center, Tokyo Institute of Technology 2-12-1 Ookayama, Meguro-ku, Tokyo, 152-8550, Japan

<sup>5</sup>National Institute for Materials Science, Tsukuba 305-0047, Japan

<sup>6</sup>Department of Physics, Faculty of Science, Yamaguchi University, 1677-1 Yoshida, Yamaguchi 753-8512, Japan

<sup>7</sup>NIMS Beamline Station at SPring-8, National Institute for Materials Science, Sayo, Hyogo 679-5148, Japan

### Abstract

The structural phase transitions of  $\text{Rb}_2\text{MoO}_4$  and  $\text{Rb}_2\text{WO}_4$  have been reinvestigated with the use of heat capacity measurement and synchrotron X-ray and neutron scattering techniques. In  $\text{Rb}_2\text{MoO}_4$ , the existence of polymorphous structures has been confirmed. These crystal structures at 290 K are a monoclinic  $\beta\text{-K}_2\text{MoO}_4$  type one and an orthorhombic  $\beta\text{-K}_2\text{SO}_4$  type one. In an annealed sample, two typical first-order-type anomalies were observed at 783 and 752 K. Furthermore, new  $\lambda$ -type anomaly equivalent to the second normal-incommensurate phase transition in  $\text{A}_2\text{BO}_4$ -type ferroelectrics was observed at 223 K. On the other hand, the crystal structure at 290 K of  $\text{Rb}_2\text{WO}_4$  was a monoclinic  $\beta\text{-K}_2\text{MoO}_4$  type one and no phase transition was detected down to 8 K.

Key word:  $\text{Rb}_2\text{MoO}_4$ ,  $\text{Rb}_2\text{WO}_4$ , structural phase transition, structural analysis

### I. Introduction

Many of the  $\text{A}_2\text{BO}_4$ -type crystals have the  $\beta\text{-K}_2\text{SO}_4$  type structure (space group  $Pnam$ ). Since the subgroup  $Pna2_1$  is polar, the family of crystal has been investigated widely as a candidate of ferroelectrics. However, these crystals have not necessarily the same succession of the phase transition. According to an empirical rule about the ratio the ionic radius of  $\text{A}^+$  to the average bond length B-O in the  $\text{BO}_4^{2-}$  tetrahedron,  $r(\text{A})/r(\text{BO})$  [1],  $\text{A}_2\text{BO}_4$ -type crystals can be loosely classified into two main groups. When the ratio is less than 1.3 beyond 0.93 (group I), all compounds transform from the parent high-symmetry hexagonal phase (phase I,  $\alpha\text{-K}_2\text{SO}_4$  type, space group  $P6_3/mmc$ ) to the orthorhombic phase (phase II,  $\beta\text{-K}_2\text{SO}_4$  type,  $Pnam$ , normal,  $Z=4$ ,  $a_0$ ,  $b_0$ ,  $c_0$ ) at high temperatures ( $T_{\text{I-II}} = 700 \sim 1100$  K), for example  $\text{A}_2\text{CrO}_4$ ,  $\text{A}_2\text{SO}_4$ ,  $\text{Rb}_2\text{SeO}_4$ ,  $\text{Cs}_2\text{SeO}_4$  and  $\text{Cs}_2\text{MoO}_4$  ( $\text{A}=\text{K}$ ,  $\text{Rb}$  and  $\text{Cs}$ ) [2]. When the ratio is under 0.93 (group II), there is another intermediate high-temperature incommensurate phase between phases I ( $\alpha\text{-K}_2\text{SO}_4$  type,  $P6_3/mmc$ ) and II

( $\beta\text{-K}_2\text{MoO}_4$  type,  $C2/m$ ), for example  $\text{K}_2\text{WO}_4$  and  $\text{K}_2\text{MoO}_4$  [3]. Although it is reported that  $\text{Rb}_2\text{MoO}_4$  and  $\text{Rb}_2\text{WO}_4$  have the monoclinic  $\beta\text{-K}_2\text{MoO}_4$  type structures at room temperature and some phase transitions, at 503 and 773 K for  $\text{Rb}_2\text{MoO}_4$  and at 568, 663 and 738 K for  $\text{Rb}_2\text{WO}_4$ , it has not clarified fully yet [4, 5].

Among the  $\text{A}_2\text{BO}_4$ -type crystals belonging to the group I, the low-temperature normal-incommensurate (N-INC) phase was observed only in  $\text{K}_2\text{SeO}_4$ . As temperature decreases  $\text{K}_2\text{SeO}_4$  transforms from phase I to phase II and to a low-temperature incommensurate phase (phase III,  $\sim 3a_0$ ,  $b_0$ ,  $c_0$ ), which is followed by a ferroelectric phase (phase IV,  $Pna2_1$ ,  $Z=12$ ,  $3a_0$ ,  $b_0$ ,  $c_0$ ) [6]. In the case of  $\text{K}_2\text{CrO}_4$  and  $\text{Rb}_2\text{SeO}_4$ , the calculated dispersion curves contain an unstable  $\Sigma_2$  phonon branch [7], which is similar to those obtained for the prototype incommensurate material  $\text{K}_2\text{SeO}_4$ . But no transition is detected down to 0 K in  $\text{K}_2\text{CrO}_4$  and  $\text{Rb}_2\text{SeO}_4$ . The calculated temperatures of hypothetical phase transitions are 4 K and -7 K for  $\text{K}_2\text{CrO}_4$  and  $\text{Rb}_2\text{SeO}_4$ , respectively. However, a softening tendency of the  $\Sigma_2$  phonon branch

around  $0.7a^*$  was observed in  $K_2CrO_4$  [8] and  $Rb_2SeO_4$  [2].

We have been studying the mechanism of normal-incommensurate phase transition and hypothetical one in  $A_2BO_4$ -type crystals. In  $Rb_2MoO_4$  and  $Rb_2WO_4$ , because the value of  $r(A)/r(BO)$  is nearly identical to 0.93, it was expected that the N-INC phase transition exists as similar to  $K_2SeO_4$ . In order to obtain additional information about structures and structural phase transitions in  $Rb_2MoO_4$  and  $Rb_2WO_4$ , we performed heat capacity measurement, and synchrotron X-ray and neutron scattering experiments. The observed results and discussions are presented in the following.

## II. Experimental

Powder samples of  $Rb_2MoO_4$  and  $Rb_2WO_4$  were prepared by the solid-state reaction method in air at 900 K for 24 hours using  $Rb_2CO_3$ ,  $MoO_3$  and  $WO_3$  as starting materials. Furthermore, single crystals of  $Rb_2MoO_4$  were grown by a slow evaporation method from a saturated ammonium solution of  $Rb_2CO_3$  and  $MoO_3$  at 310 K. By a preliminary X-ray diffraction analysis, crystal systems for powder samples and single crystal samples in  $Rb_2MoO_4$  were confirmed orthorhombic and monoclinic, respectively. Single crystal samples were annealed in air at 500 K for 4 hours before measurements in order to get the orthorhombic morphotype.

A heat capacity measurement was carried out by using a heat capacity measurement module, Quantum Design PPMS, in the temperature range from 2 to 300 K. Above 300 K, different scanning calorimeter (DSC) measurement was carried out on a SEIKO DSC220 at a heating rate  $5 \text{ Kmin}^{-1}$ . The heat capacity of the empty calorimeter in DSC was calibrated by the use of sapphire as a standard sample.

X-ray powder diffraction measurements with a large Debye-Scherrer camera were performed using the synchrotron radiation source at the BL15XU beam line of SPring-8 [9]. Incident beam was monochromatized at  $\lambda = 0.65297 \text{ \AA}$ . Neutron powder diffraction experiments were also performed by using the Kinken powder diffractometer for high efficiency and high resolution measurements, HERMES, of Institute for Materials Research, Tohoku University, installed at the JRR-3M reactor in Japan Atomic Energy Research Institute (JAERI), Tokai [10]. Neutrons with a wavelength of  $1.8196 \text{ \AA}$  were obtained by the 331 reflection of a Ge monochromator. These diffraction data were analyzed using the Rietveld method (RIETAN-FP) [11].

## III. Results and discussion

Figure 1 shows X-ray powder diffraction patterns of annealed  $Rb_2MoO_4$  at 290 K. Although the crystal structure of non-annealed sample is the monoclinic  $\beta\text{-K}_2\text{MoO}_4$  type, the crystal structure of annealed sample is orthorhombic ( $\beta\text{-K}_2\text{SeO}_4$  type structure, space group  $Pnam$ ). The orthorhombic structural parameters were refined by least-squared calculations, and final results are given in Table 1. The  $R$ -factors  $R_{wp}$  (weighted pattern  $R$ -factor),  $R_p$  (pattern  $R$ -factor) and  $R_e$  (expected  $R$ -factor) are 6.65 %, 4.78 % and 0.27 %, respectively. The value of  $r(A)/r(BO)$  is determined as 0.943, with using the ionic radius of  $A^+$  (8-coordinated site)  $1.61 \text{ \AA}$  and  $A^+$  (11-coordinated site)  $1.69 \text{ \AA}$  [12], and the bond lengths B-O in the tetrahedral  $BO_4^{2-}$  ion  $1.724(5)$ ,  $1.735(5)$ ,  $1.771(8)$  and  $1.771(8) \text{ \AA}$ . Below  $T_3$  (about 230 K) the superlattice reflections appeared at the position  $(\sim h/3, k, l)$ , where  $h, k$  and  $l$  denote the Miller indices in the normal phase ( $T_3 < T < T_2$ ), similar to  $K_2SeO_4$  (group I). Therefore, the low-temperature phase transition at  $T_3$  is a N-INC phase one. Among  $A_2BO_4$  crystals, annealed  $Rb_2MoO_4$  is the second example that possesses the N-INC phase transition. At 290 K, it has been confirmed that the crystal prepared by the solid-state reaction method is orthorhombic  $\beta\text{-K}_2\text{SO}_4$  type structure.

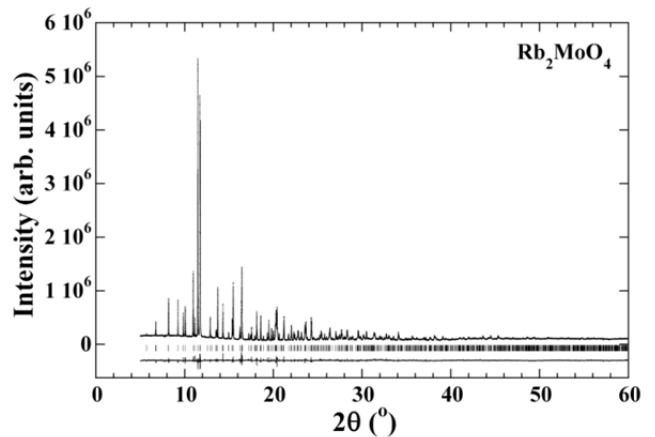


Fig. 1 X-ray powder diffraction patterns of annealed  $Rb_2MoO_4$  at 290 K. The positions shown by dot-marks represent observed diffraction data. The continuous solid-line is the calculated profile from Rietveld refinement, and small vertical markers show the positions of all the allowed Bragg reflections in the  $Pnam$  space group of  $Rb_2MoO_4$ . The lower curve represents the difference between the observed and the calculated profiles.

Figure 2 shows the molar heat capacity measured in the annealed sample of  $Rb_2MoO_4$ . Two anomalies due to the high-temperature phase transitions are observed at  $T_1 = 783$  and  $T_2 = 752$  K, such as  $K_2WO_4$

and  $\text{K}_2\text{MoO}_4$  (group II), which are very sharp and of first-order nature. The entropies of transition  $\Delta S_1$  and  $\Delta S_2$ , and the enthalpies of transition  $\Delta H_1$  and  $\Delta H_2$  are estimated to be  $4.11 \text{ Jmol}^{-1}\text{K}^{-1}$ ,  $3.88 \text{ Jmol}^{-1}\text{K}^{-1}$ ,  $3.22 \text{ kJmol}^{-1}$  and  $2.92 \text{ kJmol}^{-1}$ , respectively. Furthermore,  $\lambda$ -type anomaly was also observed at  $T_3 = 223 \text{ K}$  ( $\Delta S_3 = 1.043 \text{ Jmol}^{-1}\text{K}^{-1}$ ,  $\Delta H_3 = 0.229 \text{ kJmol}^{-1}$ ). The transition points reported around 503 and 773 K was not confirmed by our study both crystals grown by the solid-state reaction method and the slow evaporation method.

Table 1 Final positional parameters and isotropic atomic displacement parameters of annealed  $\text{Rb}_2\text{MoO}_4$  at 290 K: Space group;  $Pnam$ .  $a_0 = 8.0926(1) \text{ \AA}$ ,  $b_0 = 11.0998(1) \text{ \AA}$ ,  $c_0 = 6.3739(1) \text{ \AA}$  and  $V = 572.536(9) \text{ \AA}^3$ .

Atom	x	y	z	B( $\text{\AA}^2$ )
Rb1	0.6687(1)	0.4198(1)	0.25	2.21(4)
Rb2	0.9987(2)	0.7104(1)	0.25	2.13(4)
Mo	0.2185(1)	0.4210(2)	0.25	1.22(3)
O1	0.0058(8)	0.4297(7)	0.25	4.32(20)
O2	0.3130(9)	0.5613(7)	0.25	2.99(18)
O3	0.2830(6)	0.3442(6)	0.0206(10)	3.35(20)

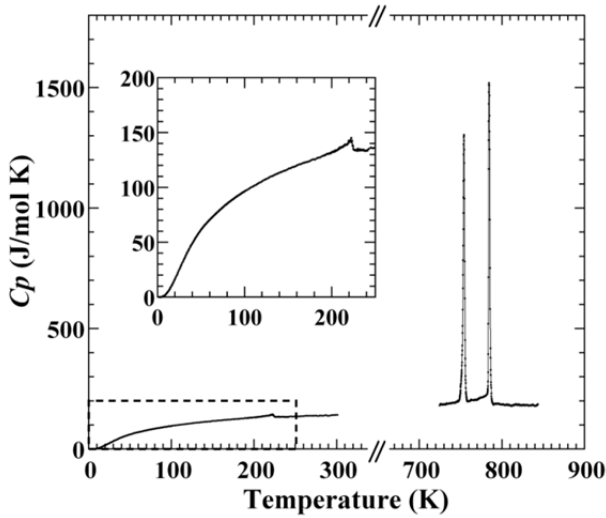


Fig. 2 Molar heat capacity measured in annealed  $\text{Rb}_2\text{MoO}_4$ .

On the other hand, at room temperature  $\text{Rb}_2\text{WO}_4$  takes monoclinic  $\beta\text{-K}_2\text{MoO}_4$  structure (space group  $C2/m$ ), which retains down to 8 K. The  $R$ -factors at 290 K obtained were as follows;  $R_{\text{wp}}$  5.37 %,  $R_p$  4.15 %, and  $R_e$  3.34 %, respectively. The value of  $r(\text{A})/r(\text{BO})$  in determined as 0.926. Neutron powder diffraction patterns and the final structural parameters are shown in Figure 3 and Table 2, respectively.

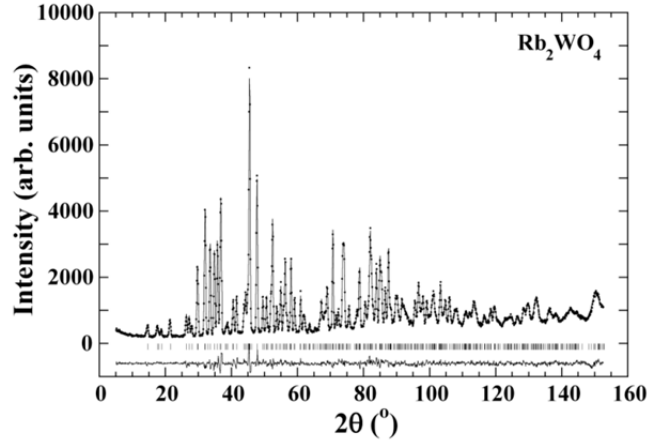


Fig. 3 Neutron powder diffraction patterns of  $\text{Rb}_2\text{WO}_4$  at 290 K. The positions shown by dot-marks represent observed diffraction data. The continuous solid-line is the calculated profile from Rietveld refinement, and small vertical markers show the positions of all the allowed Bragg reflections in the  $C2/m$  space group of  $\text{Rb}_2\text{WO}_4$ . The lower curve represents the difference between the observed and the calculated profiles.

Table 2 Final positional parameters and isotropic atomic displacement parameters of  $\text{Rb}_2\text{WO}_4$  at 290 K: Space group;  $C2/m$ .  $a = 12.8338(5) \text{ \AA}$ ,  $b = 6.2827(2) \text{ \AA}$ ,  $c = 7.8505(3) \text{ \AA}$ ,  $\beta = 115.794(2)$  and  $V = 569.92(77)$ .

Atom	x	y	z	B( $\text{\AA}^2$ )
Rb1	0.5088(3)	0	0.2367(4)	1.56(8)
Rb2	0.8442(3)	0	0.2572(4)	2.04(8)
W	0.1761(4)	0	0.2256(6)	1.56(11)
O1	0.3255(3)	0	0.3760(5)	2.19(10)
O2	0.0903(3)	0	0.3533(5)	2.15(9)
O3	0.1429(2)	0.2312(4)	0.0807(3)	1.88(8)

Here, lattice parameters ratio  $a_0/c_0$  in the  $\beta\text{-K}_2\text{SO}_4$  type structure are adopted as an additional parameters for the group I, where the  $a$ -axis is a pseudo-hexagonal axis and  $b_0 \cong \sqrt{3}c_0$ . In fact, the value of  $a_0/c_0$  for our annealed  $\text{Rb}_2\text{MoO}_4$  are determined as 1.270. According to the rigid body motion analysis and Brown theory [13, 14], A(1) (11-coordinated site) ion is the main one that produces the different type of transitions, and the rotation of the tetrahedral  $\text{BO}_4^{2-}$  ion around the  $c$ -axis is important to remain the orthorhombic  $\beta\text{-K}_2\text{SO}_4$  type structure. The rotation contributes to change the lattice parameter ratios  $a_0/c_0$  ( $\cong \sqrt{3}a_0 / b_0$ ) and  $a_0/b_0$ . Figure 4 shows the relationship between lattice parameter ratios  $a_0/c_0$  and phase transition temperatures of representative  $\text{A}_2\text{BO}_4$ -type crystals, which belong to the group I. The values obtained for  $a_0/c_0$  and  $T_3$  are 1.270 and 223 K in

annealed  $\text{Rb}_2\text{MoO}_4$ , 1.277 and 131 K in  $\text{K}_2\text{SeO}_4$ , 1.297 and 4 K in  $\text{K}_2\text{CrO}_4$ , 1.292 and -7 K in  $\text{Rb}_2\text{SeO}_4$ , and 1.302 and -111 K in  $\text{Cs}_2\text{SeO}_4$ , respectively. The N-INC phase transition temperature increases loosely with decreasing lattice parameter ratio  $a_0/c_0$ .

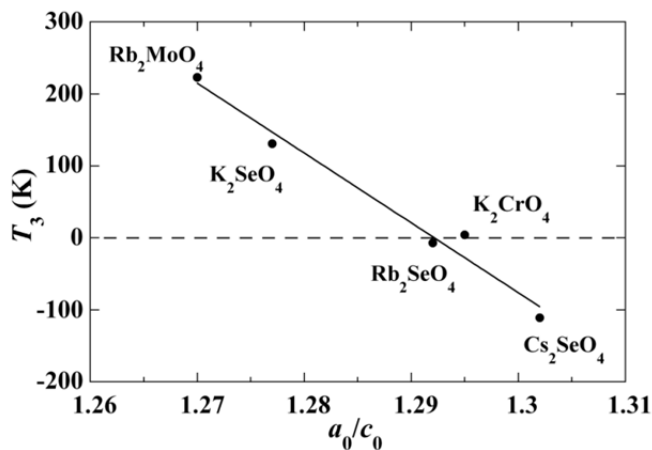


Fig. 4 The relationship between the lattice parameter ratios  $a_0/c_0$  and the N-INC phase transition temperatures of some  $\text{A}_2\text{BO}_4$ -type crystals belonging to the group I. Here, the temperature 4 K for  $\text{K}_2\text{CrO}_4$ , -7 K for  $\text{Rb}_2\text{SeO}_4$  and -111 K for  $\text{Cs}_2\text{SeO}_4$  are calculated values in ref 7. The existence of the transition in  $\text{K}_2\text{CrO}_4$  was not confirmed by experimental studies in ref 8.

In conclusion,  $\text{A}_2\text{BO}_4$ -type crystals can be classified by both ratios of  $r(\text{A})/r(\text{BO})$  and  $a_0/c_0$ . Annealed  $\text{Rb}_2\text{MoO}_4$  has both characters of groups I and II and is expected to undergo the succession of phase transition: the high-symmetry hexagonal phase ( $\alpha$ - $\text{K}_2\text{SO}_4$  type) – intermediate high-temperature incommensurate phase – orthorhombic phase ( $\beta$ - $\text{K}_2\text{SO}_4$  type) – low-temperature incommensurate phase. Unfortunately, it is not clear the connection between another room temperature phase (monoclinic  $\beta$ - $\text{K}_2\text{MoO}_4$  type) and the suggested successive phase transition. In annealed  $\text{Rb}_2\text{MoO}_4$ , the new phase transition at  $T_3$  is considered as a displacive-type transition with a typical soft phonon mode. Furthermore, the existence of a lock-in transition below  $T_3$  can be expected, so the inelastic neutron scattering and X-ray scattering studies are now in progress.

## Acknowledgment

The present work was partly supported by the collaborative research project of Materials and Structures Laboratory, Tokyo Institute of Technology, and by a research grant from the Yamaguchi University Foundation.

## References

- [1] For example, H. Mashiyama, M. Takesada, M. Kojima and H. Kasano, *Ferroelectrics* **152**, 313 (1994).
- [2] H. Shigematsu, Y. Akishige, H. Mashiyama, T. Tojo, H. Kawaji, T. Atate and T. Matsui, *J. Korean Phys. Soc.* **46**, 235 (2005).
- [3] A. Jorio, P. Saint-Gregoire and M. A. Pimenta, *J. Phys.: Condens. Matter* **12**, 9307 (2000).
- [4] A. W. M. Van Den Akker, A. S. Koster and G. D. Rieck, *J. Appl. Cryst.* **3**, 389 (1970).
- [5] F. X. N. M. Kools, A. S. Koster and G. D. Rieck, *Acta Crystallogr. B* **26**, 1974 (1970).
- [6] J. D. Axe, M. Iizumi and G. Shirane, *Phys. Rev. B* **22**, 3408 (1980).
- [7] I. Etxebarria, J. M. Perez-Mato and G. Madariaga, *Phys. Rev. B* **46**, 2764 (1992).
- [8] I. Etxebarria, M. Quilichini, J. M. Perez-Mato, P. Boutrouille, F. J. Zuniga and T. Brezowski, *J. Phys.: Condens. Matter* **4**, 8551 (1992).
- [9] M. Tanaka, Y. Katsuya and A. Yamamoto, *Rev. Sci. Instrum.* **79**, 075106 (2008).
- [10] K. Ohoyama, T. Kanouchi, K. Nemoto, M. Ohashi, T. Kajitani and Y. Yamaguchi *Jpn. J. Appl. Phys.* **37**, 3319 (1998).
- [11] F. Izumi and T. Ikeda, *Mater. Sci. Forum* **321-324**, 198 (2000).
- [12] R. D. Shano, *Acta Crystallogr. A* **32**, 751 (1976).
- [13] I. D. Brown, *Acta Crystallogr. B* **48**, 553 (1992).
- [14] X. Solans, C. Ruiz-Perez, C. Gonzalez-Silgo, L. Mestres, M. L. Martinez-Sarrion and E. Bocanegra: *J. Phys.: Condens. Matter* **10**, 5245 (1998).